Nonequilibrium Casimir Force with a Nonzero Chemical Potential for Photons

Kaifeng Chen and Shanhui Fan

Phys. Rev. Lett. **117**, 267401 — Published 22 December 2016

DOI: 10.1103/PhysRevLett.117.267401

Non-equilibrium Casimir force with a non-zero chemical potential for photons

Kaifeng Chen[1,2] and Shanhui Fan[a2]

[1] *Department of Applied Physics, Stanford University, California 94305, USA*

[2] *Department of Electrical Engineering, Ginzton Laboratory, Stanford University, Stanford, California 94305, USA*

(Dated: November 17, 2016)

Abstract

We introduce a new class of non-equilibrium Casimir forces, where the deviation from equilibrium is achieved through the use of non-zero chemical potential of photons. Such a force can be observed when two semiconductors are brought in close proximity to each other, and when at least one of the semiconductors are subject to an external voltage. By exact numerical calculations of a sphere-plate configuration, we show that in the total force the non-equilibrium component can dominate over its equilibrium counterpart with a relatively modest external voltage, even when the sphere-plate separation is in the nanoscale. And as a result, repulsion can be achieved at nanoscale even with relatively modest applied voltage. The results here point to a pathway that can significantly advance the quest for observing and harnessing non-equilibrium Casimir forces in solid-state systems.

[a] shanhui@stanford.edu

The study of non-equilibrium Casimir forces represents an emerging direction in the explorations of physical effects induced by quantum and thermal fluctuations [1–9]. In the standard configuration for the study of non-equilibrium Casimir forces, one considers two bodies maintained at different temperatures, and studies the forces that are generated by the quantum and thermal fluctuations in each of the bodies. This is in contrast to the equilibrium Casimir forces that have been extensively studied [10–21] since the pioneering works of Casimir [22] and Liftshitz [23], where the bodies are maintained at the same temperature.

The non-equilibrium situation creates fundamentally different physical effects in fluctuation-induced forces. For example, whereas the equilibrium Casimir forces between two bodies are almost always attractive except with unusual geometries [24, 25] or material systems [26, 27], it has been shown theoretically that even with regular material systems and geometries the non-equilibrium force can be repulsive, and may provide stable equilibrium points [1, 2]. From a practical point of view, having a repulsive interaction is important in nanoelectromechanical systems for preventing the collapse of nanostructures [20, 28]. In addition, moving away from equilibrium points to a new dimension in controlling fluctuation-induced forces. For example, In the non-equilibrium case one can control the force by changing the temperature gradient.

In spite of the importance of non-equilibrium Casimir forces for fundamental science and practical applications, observation of such forces has proved to be quite challenging. At small separations, the fluctuation force is dominated by its equilibrium component. To observe non-equilibrium effect, the distance needs to be at least comparable to the thermal wavelength. At such distance, the magnitude of the total fluctuation force however becomes quite small, which presents a significant experimental difficulty. As a result, the only existing observations of such forces were carried out on atomic systems [9]. There have not been any experiments on non-equilibrium forces in solid-state systems that are important for practical applications. Moreover, as has been pointed out in Ref. [3], to observe a repulsive interaction between a metallic sphere and a metallic substrate requires a very large temperature difference of more than 600 K, and moreover the repulsion occurs only at a relatively large micron-scale distances. And yet for nanomechanical applications it would be far more attractive to be able to achieve repulsive interaction at nanoscale.

Motivated by the goal to harness the fluctuation-induced forces, in this Letter we propose a class of non-equilibrium Casimir forces that occurs between two bodies possessing

different chemical potential for photons. When a semiconductor is under an external voltage bias, the electromagnetic fluctuations of the semiconductor can acquire a non-zero chemical potential proportional to the applied voltage [29–32]. Here we consider two semiconductors subject to different voltages, and show that the control of such external voltage provides a powerful mechanism to harness the fluctuation-induced forces. We show that in this geometry, the non-equilibrium force exceeds the equilibrium component even when the spacing is at nanoscale, and thus in this case, the non-equilibrium Casimir force is sufficiently large to facilitate experimental observations. In addition, we show that the forces between the bodies can become repulsive with modest contrast in chemical potentials even at nanoscale dimension. This represents a capability to achieve repulsion that is beyond what has been possible in standard temperature-based non-equilibrium Casimir forces.

The Casimi-Lifshitz forces arise from the quantum and thermal fluctuations of the system. In a semiconductor under external bias V maintained at temperature T, for the angular frequencies above and below the bandgap, the correlations of the fluctuation currents inside the body are assumed to have the following form [31–34]

$$\langle \boldsymbol{j}_\alpha(\boldsymbol{r},\omega)\boldsymbol{j}^*_\beta(\boldsymbol{r}',\omega')\rangle = \begin{cases} \left(\frac{1}{2}+\frac{1}{e^{\frac{\hbar\omega-qV}{k_BT}}-1}\right)\frac{4}{\pi}\hbar\omega^2\epsilon''(\omega)\delta(\boldsymbol{r}-\boldsymbol{r}')\delta(\omega-\omega')\delta_{\alpha\beta} & (\omega\geq\omega_g) \\ \left(\frac{1}{2}+\frac{1}{e^{\frac{\hbar\omega}{k_BT}}-1}\right)\frac{4}{\pi}\hbar\omega^2\epsilon''(\omega)\delta(\boldsymbol{r}-\boldsymbol{r}')\delta(\omega-\omega')\delta_{\alpha\beta} & (\omega<\omega_g), \end{cases}$$

(1a)

(1b)

where ω and ω' are the angular frequencies, $\hbar$ is the reduced Planck constant, k_B is the Boltzmann constant, α and β label the directions of polarization, $\boldsymbol{r}$ and $\boldsymbol{r'}$ are position vectors and $\delta(\omega-\omega')$ is the Dirac delta function, ω_g is the bandgap angular frequency. For angular frequencies above the bandgap, the current-current correlation is dependent of the external bias V on the semiconductor p-n junction. While for angular frequencies below the bandgap, the correlation function reduces to a more commonly used form with $V=0$, as is shown in Eq. 1b. For such a semiconductor, both Eqs. 1a and 1b can be separated into a T-independent term that describes the zero-point quantum fluctuation, and a T-dependent term that describes the thermal fluctuation.

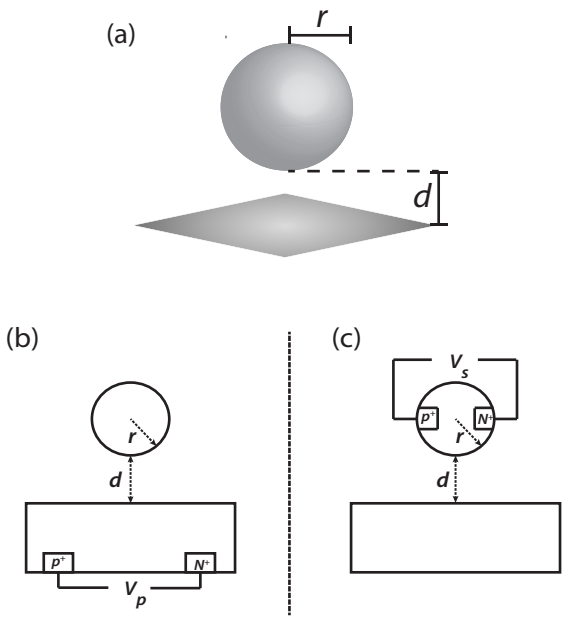

FIG. 1. (a) Configuration of a system consisting of a sphere and a semi-infinite plate. The sphere has radius r and the distance between the bottom of the sphere and the plate is d. (b) An external bias V_p is applied on the p-n junction in the semiconductor plate. (c) An external bias V_s is applied on the p-n junction in the semiconductor sphere.

The Casimir force is obtained by calculating the Maxwell stress tensor induced by above-bandgap and below-bandgap fluctuations. From Eq. 1a, by applying the external bias V, one can thus control the contribution to the non-equilibrium Casimir forces from the above-bandgap radiation. To demonstrate the effects created by an external bias, in this Letter, we consider the sphere-plate geometry since such configuration is commonly used in experiments [35, 36] and has been numerically computed by using proximity force approximation [37] or exact calculations using scattering theory [2, 3, 38–41]. As is shown in Fig. 1 (a), the system contains a sphere with radius r and a semi-infinite plate, and the distance from the bottom of the sphere to the plate is d. Throughout the paper, we denote the sphere as s and the plate as p in super or subscripts. We denote the temperatures of the sphere, the plate and the environment as T_s, T_p and $T_{\rm env}$, respectively.

In Figs. 1 (b) and (c), we consider two scenarios of using an external bias to control the non-equilibrium Casimir force. In Fig. 1 (b), we consider the case when the plate is made of a semiconductor, and a bias is applied to contacts at P^+ and N^+ regions. In the presence

of the bias V_p, using the scattering theory formalism as developed in [3] and noting that the only change in the formalism is the replacement of the equilibrium photon occupation number by a non-equilibrium one, the total force acting on the sphere $\mathbf{F}^s$ is

$$\mathbf{F}^s = \mathbf{F}^{(s,\mathrm{eq})}(T_{\mathrm{env}}) + \left[\mathbf{F}^s_p(T_p, V_p) - \mathbf{F}^s_p(T_{\mathrm{env}})\right]^+ + \left[\mathbf{F}^s_p(T_p) - \mathbf{F}^s_p(T_{\mathrm{env}})\right]^- + \left[\mathbf{F}^s_s(T_s) - \mathbf{F}^s_s(T_{\mathrm{env}})\right]. \tag{2}$$

The first term describes the equilibrium force and the remaining terms describe the non-equilibrium forces. In the remaining terms, the superscript of a force term represents the body where the force is exerted upon, and the subscript represents the fluctuating sources that generate such force. For example, $\mathbf{F}^s_p$ corresponds to the force on the sphere, due to the fluctuations in the plate. The second term in Eq. 2 describes the contribution to the non-equilibrium Casimir force from the above-bandgap radiation (denoted using superscript "+"), and is controlled by V_p. The third term in Eq. 2 represents the contribution from the sub-bangap radiation (denoted using superscript "−"). The last term describes the contribution from the thermal fluctuations in the sphere because of the difference between T_s and T_{env}. In Fig. 1 (c), we consider an alternative case where the sphere is subject to an external bias V_s applied to contacts at its P^+ and N^+ regions. In this case, the total force on the sphere is

$$\mathbf{F}^s = \mathbf{F}^{(s,\mathrm{eq})}(T_{\mathrm{env}}) + \left[\mathbf{F}^s_p(T_p) - \mathbf{F}^s_p(T_{\mathrm{env}})\right] + \left[\mathbf{F}^s_s(T_s, V_s) - \mathbf{F}^s_s(T_{\mathrm{env}})\right]^+ + \left[\mathbf{F}^s_s(T_s) - \mathbf{F}^s_s(T_{\mathrm{env}})\right]^-. \tag{3}$$

With $V_p = 0$ or $V_s = 0$, Eq. 2 or 3 reproduce the standard formula for non-equilibrium Casimir forces, respectively. The explicit form of various terms in Eqs. 2 and 3 are provided in Supplementary Material.

Eqs. 2 and 3 are applicable to the general non-equilibrium case, where there can be temperature differences for the bodies and the environments, as well as voltage difference between the bodies. For the rest of the paper, to highlight the effect of the voltage difference, we will consider only the case where $T_s = T_p = T_{\mathrm{env}} \equiv T$. In such a case, Eqs. 2 and 3 are simplified to:

$$\mathbf{F}^s = \mathbf{F}^{(s,\mathrm{eq})} + \left[\mathbf{F}^s_p(V_p) - \mathbf{F}^s_p\right]^+, \tag{4}$$

and

$$\mathbf{F}^s = \mathbf{F}^{(s,\mathrm{eq})} + \left[\mathbf{F}^s_s(V_s) - \mathbf{F}^s_s\right]^+. \tag{5}$$

In Eqs. 4 and 5, as well as for the rest of the paper, the dependency on T is now implicit since all bodies have the same temperature. Note that in this case, the only contribution to the non-equilibrium force comes from radiation above the band gap energy.

Using Eqs. 4 and 5, we perform numerically exact calculations on the systems shown in Figs. 1 (b) and (c), and compute the equilibrium Casimir force and non-equilibrium Casimir force separately. Throughout the paper, we set $T = 300$ K. For the equilibrium force, i.e. $\mathbf{F}^{(s,\mathrm{eq})}$, following Ref. [39], we perform Wick rotation when integrating over the angular frequencies. The non-equilibrium forces in Eqs. 2 and 3 are obtained using the trace formula introduced in [3] which relates the forces to the traces of the appropriate field correlators. In the numerical calculations, to ensure convergence, we use the criteria given in [42] in the summation over different angular momentum channels.

Since in the far field the Casmir force can be viewed as a result of radiative pressure [43], one would prefer to use a material with good light emitting property. Moreover, motivated by experiments with sphere-plate geometry that typically measure the forces on the sphere [35, 36], we will be primarily interested in the force on the sphere. To ensure absorption of the photons emitted from the plate, we use a semiconductor with a slightly smaller bandgap as the material for the sphere. In our calculations, we choose GaAs as the semiconductor for the plate and InP for the sphere. The bandgap of GaAs is 1.42 eV at 300 K, while InP has a bandgap of 1.34 eV. The dielectric functions for GaAs and InP for the angular frequencies above the bandgap are obtained from [44]. For sub-bandgap dielectric function, we use Lorentz-Drude model with the form of $\epsilon(\omega) = \epsilon_\infty(\omega^2 - \omega_L^2 + i\gamma\omega)/(\omega^2 - \omega_T^2 + i\gamma\omega)$ to take into account the contributions from phonon-polaritons. For GaAs, ω_T and ω_L correspond to energies of 0.0333 eV, 0.0362 eV, respectively and $\epsilon_\infty = 11.0$, $\gamma = 4.52 \times 10^{11}$ rad/s [44]. For InP, ω_T and ω_L correspond to energies of 0.0377 eV, 0.0428 eV, respectively and $\epsilon_\infty = 9.61$ and $\gamma = 6.59 \times 10^{11}$ rad/s [44]. The radius of the sphere r is fixed to be 1 μm.

We first consider the configuration in Fig. 1 (b). We plot the equilibrium Casimir force $\mathbf{F}^{s,\mathrm{eq}}$, the non-equilibrium Casimir force $\Delta\mathbf{F}_p^s = [\mathbf{F}_p^s(V_p) - \mathbf{F}_p^s]^+$, and the total force on the sphere $\mathbf{F}^s$ in the presence of bias $V_p = 1.36$ V as a function of d from 10 nm to 5 μm in Fig. 2 (a) in blue, green and red curves, respectively. We define the force to be positive when it is attractive. For this system, the equilibrium component, $\mathbf{F}^{(\mathrm{s,eq})}$, is always attractive. At small d, the equilibrium component dominates and the total force is attractive. As d increases, the equilibrium component decreases rapidly. At $d \geq 50$ nm, the non-equilibrium component

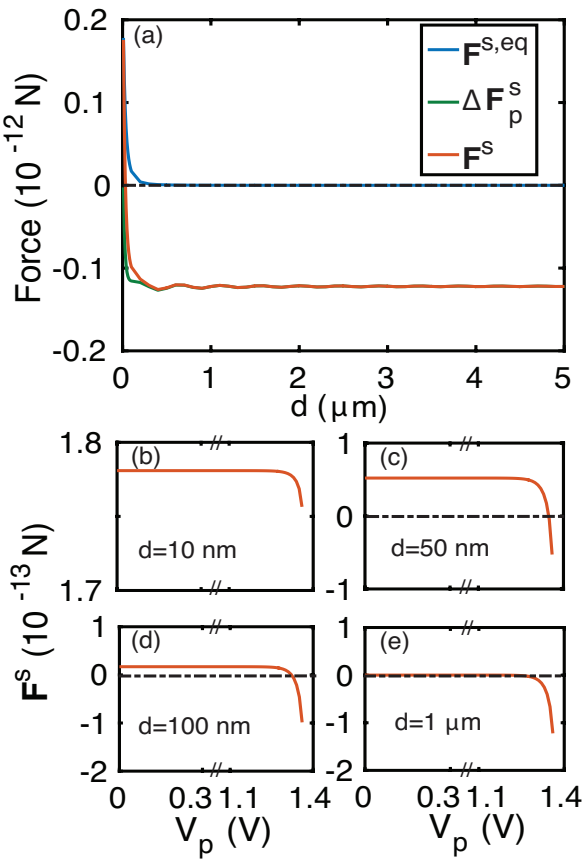

FIG. 2. (a) The equilibrium Casimir force $\mathbf{F}^{s,\mathrm{eq}}$, the non-equilibrium Casimir force $\Delta\mathbf{F}^s_p = [\mathbf{F}^s_p(V_p) - \mathbf{F}^s_p]^+$ and the total force on the sphere $\mathbf{F}^s$ for the configuration of Fig. 1 (b) as a function of d from 10 nm to 5 μm when $V_p = 1.36$ V. The dot dashed horizontal black line corresponds to $|\mathbf{F}^s| = 0$. (b)-(e) the total force on the sphere $\mathbf{F}^s$ as a function of the external bias V_p for various d values shown in the legend. The dotted-dashed horizontal black line corresponds to $|\mathbf{F}^s| = 0$.

starts to dominate, and the overall force becomes repulsive. At larger d, in the far-field limit, the total force comes entirely from its non-equilibrium component, which can also be interpreted as radiation pressure [43], and as a result the total force becomes independent of d. Therefore in this system, one can observe non-equilibrium force and repulsion at nano-scale. This is in contrast with previous works on non-equilibrium Casimir force based on temperature gradient where repulsion is achieved at micron-scale [2].

For this system, the non-equilibrium force is strongly influenced by the applied bias V_p. In Fig. 2 (c), we plot the total force as a function of applied bias when the spacing is fixed at $d = 50$ nm. When V_p is small compared to the bandgap, the total force is dominated by its

equilibrium component, and thus is attractive. However, when the external bias approaches the bandgap voltage, the non-equilibrium Casimir force is significantly enhanced, and at $V_p \geq$ 1.35 V, it dominates over the equilibrium Casimir force and results in repulsion. We further plots the total force on the sphere as a function of external bias for $d = 10$ nm, 100 nm, 1μm in Figs. 2 (b), (d) and (e), respectively. In all these cases, strong deviation of the total force from its equilibrium components occurs only when the voltage is close to the band gap. At $d = 10$ nm, the total force remains attractive for the bias range considered. At $d = 100$ nm and 1 μm, we observe the transition from attraction to repulsion as the voltage increases, and the transition occurs at a smaller voltage for larger d. In this system, repulsions are easily achieved at an external bias that is easily achievable experimentally. This is in contrast with previous works on non-equilibrium Casimir force based on temperature gradient where a large temperature difference is needed to achieve repulsion [2, 3].

The results above is for the configuration of Fig. 1 (b) where we apply an external bias on the plate. In contrast, we now instead consider the configuration in Fig. 1 (c) where an external voltage is applied to the sphere. In Fig. 3 (a), we plot the total forces acting on the sphere as d varies from 10 nm to 5 μm when a voltage of $V_s = 1.26$ V is applied on the sphere. For small separations, the equilibrium component dominates and the total force is attractive. For larger d, we observe an oscillating behavior of the total force. Mathematically, the oscillation arises from the third term in Eq. 3, which describes the self-force on the sphere, i.e. the force on the sphere due to the current fluctuations in the sphere. Physically, Such oscillations originates from the interference of the two wave components emitted from the sphere. One of these components is the emission towards the plate, which is then reflected from the plate. The other component is the emission in the direction away from the plate. In contrast to the case in Fig. 2 (a) where exhibits only one unstable equilibrium point, here the oscillation results in multiple equilibrium points where the total force is zero. These equilibrium points can be either stable or unstable as shown in Fig. 3 (a). The existence of the stable equilibrium points is a distinct feature of the non-equilibrium force for the configuration of Fig. 1 (c). Similar oscillation has been previously noted in the non-equilibrium force generated by temperature gradient [2]. In our case it is controlled by voltage rather than temperature gradient.

We further examine the dependence of the total force on V_s in Figs. 3 (b)-(e) for four different d values. For the cases $d = 10$ nm and 20 nm, as shown in Fig. 3 (b), the increase

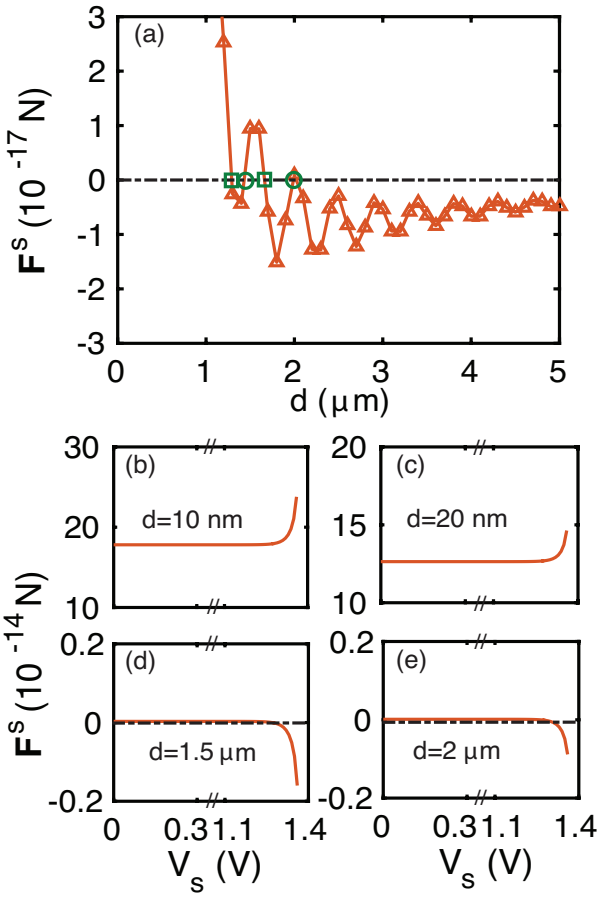

FIG. 3. (a) Total force on the sphere as a function of d for $V_s = 1.26$ V, for case (c) in Fig. 1. The dotted-dashed horizontal black line corresponds to $|\mathbf{F}^s| = 0$. Two unstable equilibrium points for are labeled using squares, and two stable equilibrium points are labeled using circles. (b)-(e) the total force on the sphere $\mathbf{F}^s$ as a function of the external bias V_s for various d values shown in the legend. The dotted-dashed horizontal black lines in (d) and (e) correspond to $|\mathbf{F}^s| = 0$.

of the voltage *enhances* the attraction of the sphere and the plate. This is in strong contrast with the case considered in Fig. 2. On the other hand, for the cases of $d = 1.5$ μm and 2 μm (Figs. 3 (d) and (e)), as V_s increases, the total force on the sphere becomes repulsive for large V_s. Due to the interference effects in the self-force of the sphere, this configuration exhibits a rich set of effects in the non-equilibrium forces as we vary either the voltage or the gap size.

In the results above, for ease of exact numerical calculations, we have chosen a relatively small sphere with a radius of 1 μm. Larger force is expected for a larger sphere. In our con-

figuration, for a sphere radius of 5 μm, repulsive force of 1.93×10^{-12} N can be achieved with a gap size of 50 nm, and with a voltage of 1.36 V applied on the plate, as can be estimated using the proximity force approximation that has been shown to be accurate for sphere of this size in this near-field regime [39]. Forces of such a magnitude is readily detectable with the current experimental techniques for the measurement of Casimir forces [45]. To summarize, we have introduced a new class of non-equilibrium Casimir forces, where the deviation from equilibrium is achieved by applying external voltages to semiconductors to create a non-zero chemical potential for photons. The use of such a chemical potential should significantly simplify the quest for observing and harnessing non-equilibrium Casimir forces in solid-state systems.

This work was supported by the DOE "Light-Material Interactions in Energy Conversion" Energy Frontier Research Center under grant DE-SC0001293.

[1] M. Krüger, T. Emig, and M. Kardar, Phys. Rev. Lett. **106**, 210404 (2011).

[2] M. Krüger, T. Emig, G. Bimonte, and M. Kardar, Europhys. Lett. **95**, 21002 (2011).

[3] M. Krüger, G. Bimonte, T. Emig, and M. Kardar, Phys. Rev. B **86**, 115423 (2012).

[4] M. Antezza, L. P. Pitaevskii, and S. Stringari, Phys. Rev. Lett. **95**, 113202 (2005).

[5] M. Antezza, L. P. Pitaevskii, S. Stringari, and V. B. Svetovoy, Phys. Rev. Lett. **97**, 223203 (2006).

[6] G. Bimonte, T. Emig, M. Krüger, and M. Kardar, Phys. Rev. A **84**, 042503 (2011).

[7] G. Bimonte, Phys. Rev. A **92**, 032116 (2015).

[8] R. Messina and M. Antezza, Europhys. Lett. **95**, 61002 (2011).

[9] J. M. Obrecht, R. J. Wild, M. Antezza, L. P. Pitaevskii, S. Stringari, and E. A. Cornell, Phys. Rev. Lett. **98**, 063201 (2007).

[10] G. L. Klimchitskaya, U. Mohideen, and V. M. Mostepanenko, Rev. Mod. Phys. **81**, 1827 (2009).

[11] F. Chen, G. L. Klimchitskaya, U. Mohideen, and V. M. Mostepanenko, Phys. Rev. Lett. **90**, 160404 (2003).

[12] B. Geyer, G. L. Klimchitskaya, and V. M. Mostepanenko, Phys. Rev. D **72**, 085009 (2005).

[13] S. A. Ellingsen, I. Brevik, J. S. Høye, and K. A. Milton, Phys. Rev. E **78**, 021117 (2008).

[14] S. K. Lamoreaux, Phys. Rev. Lett. **78**, 5 (1997).

[15] U. Mohideen and A. Roy, Phys. Rev. Lett. **81**, 4549 (1998).

[16] A. O. Sushkov, W. J. Kim, D. A. R. Dalvit, and S. K. Lamoreaux, Nat. Phys. **7**, 230 (2011).

[17] A. W. Rodriguez, F. Capasso, and S. G. Johnson, Nat. Photon. **5**, 211 (2011).

[18] A. W. Rodriguez, D. Woolf, A. P. McCauley, F. Capasso, J. D. Joannopoulos, and S. G. Johnson, Phys. Rev. Lett. **105**, 060401 (2010).

[19] J. N. Munday and F. Capasso, Phys. Rev. A **75**, 060102 (2007).

[20] H. B. Chan, V. A. Aksyuk, R. N. Kleiman, D. J. Bishop, and F. Capasso, Science **291**, 1941 (2001).

[21] M. Lisanti, D. Iannuzzi, and F. Capasso, Proc. Natl. Acad. Sci. U. S. A. **102**, 11989 (2005).

[22] H. B. G. Casimir, Proc. K. Ned. Akad. Wet. **51**, 793 (1948).

[23] E. M. Lifshitz, Sov. Phys. JETP **2**, 73 (1956).

[24] M. Levin, A. P. McCauley, A. W. Rodriguez, M. T. H. Reid, and S. G. Johnson, Phys. Rev. Lett. **105**, 090403 (2010).

[25] K. A. Milton, E. K. Abalo, P. Parashar, N. Pourtolami, I. Brevik, S. A. Ellingsen, S. Y. Buhmann, and S. Scheel, Phys. Rev. A **91**, 042510 (2015).

[26] F. Chen, G. L. Klimchitskaya, V. M. Mostepanenko, and U. Mohideen, Phys. Rev. B **76**, 035338 (2007).

[27] M. Dou, F. Lou, M. Boström, I. Brevik, and C. Persson, Phys. Rev. B **89**, 201407 (2014).

[28] E. Buks and M. L. Roukes, Nature **419**, 119 (2002).

[29] P. Wurfel, J. Phys. C **15**, 3967 (1982).

[30] P. Berdahl, J. Appl. Phys. **58**, 1369 (1985).

[31] K. Chen, P. Santhanam, S. Sandhu, L. Zhu, and S. Fan, Phys. Rev. B **91**, 134301 (2015).

[32] K. Chen, P. Santhanam, and S. Fan, Phys. Rev. Applied **6**, 024014 (2016).

[33] S. M. Rytov, *Theory of Electric Fluctuations and Thermal Radiation* (Air Force Cambridge Research Center, Bedford, MA, 1959).

[34] C. H. Henry and R. F. Kazarinov, Rev. Mod. Phys. **68**, 801 (1996).

[35] C.-C. Chang, A. A. Banishev, R. Castillo-Garza, G. L. Klimchitskaya, V. M. Mostepanenko, and U. Mohideen, Phys. Rev. B **85**, 165443 (2012).

[36] H. B. Chan, Y. Bao, J. Zou, R. A. Cirelli, F. Klemens, W. M. Mansfield, and C. S. Pai, Phys. Rev. Lett. **101**, 030401 (2008).

[37] A. Canaguier-Durand, P. A. M. Neto, A. Lambrecht, and S. Reynaud, Phys. Rev. Lett. **104**, 040403 (2010).

[38] P. A. Maia Neto, A. Lambrecht, and S. Reynaud, Phys. Rev. A **78**, 012115 (2008).

[39] R. Zandi, T. Emig, and U. Mohideen, Phys. Rev. B **81**, 195423 (2010).

[40] O. Kenneth and I. Klich, Phys. Rev. B **78**, 014103 (2008).

[41] S. J. Rahi, T. Emig, N. Graham, R. L. Jaffe, and M. Kardar, Phys. Rev. D **80**, 085021 (2009).

[42] C. R. Otey and S. Fan, Phys. Rev. B **84**, 245431 (2011).

[43] P. W. Milonni, R. J. Cook, and M. E. Goggin, Phys. Rev. A **38**, 1621 (1988).

[44] E. Palik, *Handbook of Optical Constants of Solids* (Academic, New York, 1985).

[45] G. L. Klimchitskaya, A. Roy, U. Mohideen, and V. M. Mostepanenko, Phys. Rev. A **60**, 3487 (1999).